Llopis-Lorente, A.; Lozano-Torres, B.; Bernardos Bau, A.; Martínez-Máñez, R.; Sancenón Galarza, F. (2017). Mesoporous silica materials for controlled delivery based on enzymes. Journal of Materials Chemistry B. 5(17):3069-3083. doi:10.1039/C7TB00348J

Journal Name

REVIEW

Mesoporous Silica Materials for Controlled Delivery based on Enzymes

Received 00th January 20xx,
Accepted 00th January 20xx

DOI: 10.1039/x0xx00000x

www.rsc.org/

Antoni Llopis-Lorente,[a,b,†] Beatriz Lozano-Torres,[a,b,†] Andrea Bernardos,[a,b] Ramón Martínez-Máñez,*[a,b,c] and Félix Sancenón[a,b,c]

This review summarises examples of capped mesopous silica materials for controlled delivery that uses enzymes as external triggers or functional components of the gating ensemble.

1. Introduction

The functionalisation of inorganic materials with molecular or supramolecular assemblies has recently led to the preparation of hybrid materials, within the nanoscale range in many cases, with advanced functionalities.[1,2] In fact grafting organic (bio)molecules or supramolecules onto selected inorganic solids (with different natures, sizes and shapes) has promoted the development of smart nanodevices with applications in several scientific fields.[3-7] Within the realm of functional nanodevices, one appealing concept is related with the design of gated materials. These systems are constructed for the purpose of finely tuning the movement of (bio)chemical species from the voids of porous supports to a solution in response to an external stimulus.[8] These nanodevices are generally composed of two subunits: (i) a porous inorganic support, on which a cargo is entrapped; and (ii) selected molecular and/or supramolecular entities, grafted onto the external surface, which control mass transport from the pores to the solution. In this field, one of the most widely used inorganic supports has been mesoporous silica nanoparticles,[9-12] whereas the gating mechanisms takes advantage of electrostatic or supramolecular interactions, the rupture/formation of covalent bonds, or changes in the physical properties of molecules or macromolecules.[13-21] Gated materials have found high potential applications in the field of controlled release protocols and in the development of new sensing/recognition paradigms.[22]

One of the most appealing triggers used to develop gated materials are enzymes.[8,22] For this purpose, the most commonly used enzymes are oxidoreductases, transferases, hydrolases, lipases, nucleases, phosphatases, glycosidases, lyases, isomerases and ligases. The use of enzymes for uncapping gated materials is appealing. In fact the use of tailor-made specific (bio)organic derivatives and selected enzymes is envisioned to have a huge potential, which may provide the design of advanced gated devices for delivery at will of drugs and (bio)molecules in realistic biological environments with high selectivity. Moreover, enzymes have also been used as bulky capping units.

This review intends to comprehensively analyse published papers that have used enzymes (Table 1) in combination with porous materials to design gated supports for different applications. The review is divided into two main sections that take into account the role played by the enzyme, namely (i) enzymes as functional components in the gating ensemble and (ii) enzymes as triggers (see Figure 1).

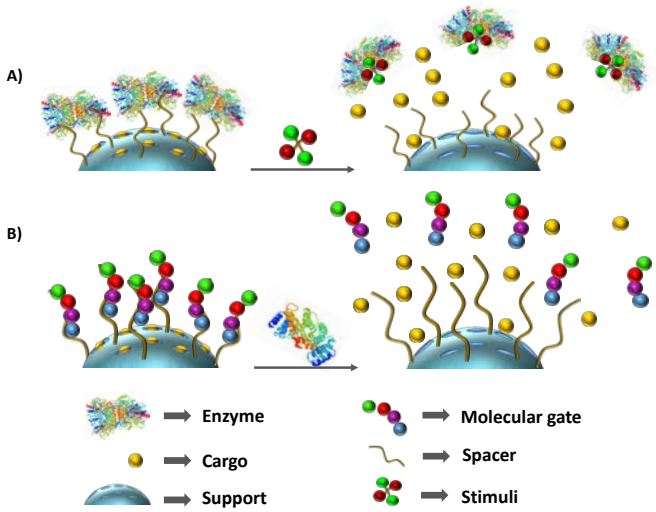

Figure 1. Schematic representation of molecular gates, for on-command controlled release, based on using enzymes. A) Enzymes are used as functional components in the gating ensemble and materials are uncapped in the presence of a certain target stimulus. B) Enzymes are used as a trigger to uncap pores via, e.g., hydrolysis or certain functional groups.

[a.] *Instituto Interuniversitario de Investigación de Reconocimiento Molecular y Desarrollo Tecnológico (IDM), Universitat Politècnica de València, Universitat de València.*
[b.] *CIBER de Bioingeniería, Biomateriales y Nanomedicina (CIBER-BBN).*
[c.] *Departmento de Química, Universitat Politècnica de València, Camí de Vera s/n, 46022 València, Spain.*
† *These authors contributed equally to this work.*

Table 1. Summary of the enzymes employed in the design of the gated delivery systems described in this review.

Enzyme	Reference
Acetylcholinesterase	34
Amidase	53-55
Acid phosphatase	67
α-Amylase	83
Carbonic anhydrase (CA)	25
Caspase	58
Catalase (CAT)	28
Cathepsin B	44-46
Cellulose glycosidase	85
α-Chymotrypsin A (CTRA)	33
DNAses	68-70
Esterase	29, 30, 59-66, 86
β-D-Galactosidase enzyme	71, 74
Glucose oxidase (GOx)	26-28, 30, 91
Glutathione S-transferase (GST)	24
Horseradish peroxidase (HRP)	91
Hyaluronidase (HAase)	76- 81
Lipase	83
Luciferase	31
Lysozyme	82
β-Mannanase	75
Metalloproteinase (MMP)	48-52
NAD(P)H:quinone oxidoreductase 1 (NQO1)	92
Pancreatin	56, 72, 73, 84
Protease	36- 43, 54
Reductase	86, 87
Telomerase	88-90
Thrombin	57
Trypsin	47
Urease	23, 32, 55

2. Enzymes as functional components

In this section, enzymes are used as components of the gating ensemble and their function in most cases is to cap the pores of the inorganic matrix. The opening and subsequent delivery of the entrapped cargo are induced using different external stimuli; e.g., presence of certain molecules or by changes in the pH of the environment.

2.1. pH triggered release

Lee and co-workers prepared pH-responsive mesoporous silica nanoparticles (MSNs) capped with urease and a calcium phosphate shell.[23] First, MSNs were functionalised with aminopropyl moieties, which were further reacted with glutaraldehyde to yield aldehyde groups on the external silica surface. Afterwards, the authors linked enzyme urease to the aldehyde groups through the formation of imine bonds. Doxorubicin (DOX) was loaded into pores and the system was closed by the enzyme-mediated formation of a calcium phosphate coating using hydroxyapatite and urea. At pH 7.4, the system remained capped, but DOX delivery was remarkable at pH 4.5 due to the dissolution of the calcium phosphate layer under acidic conditions (see Figure 2). The DOX-loaded nanoparticles were tested in MCF-7 cancer cells and induced cell death was observed due to the gradual release of DOX at the lysosomal pH.

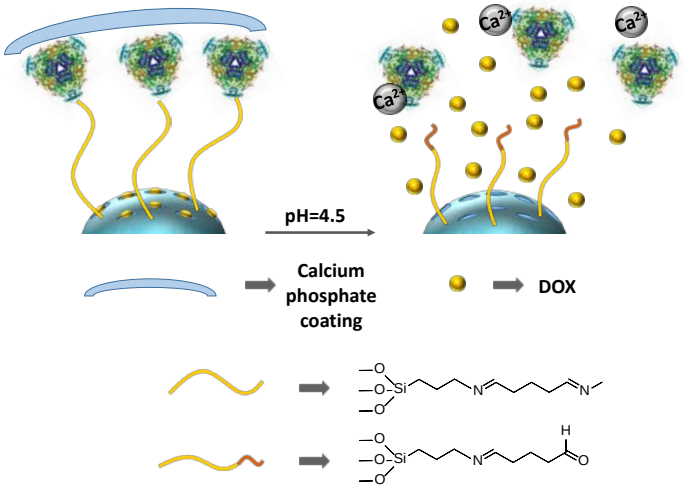

Figure 2. MSNs loaded with DOX, functionalised with urease and capped with a calcium phosphate shell. DOX was released at an acidic pH.

Chen and co-workers developed MSNs capped with glutathione S-transferase (GST) capable of cargo delivery using pH changes and glutathione as triggers.[24] The external surface of MSNs was functionalised with (3-aminopropyl)triethoxysilane (APTES), followed by the encapsulation of rhodamine 6G (Rh 6G) or DOX inside the inorganic scaffold pores. Finally, the system was capped by GST, which interacted electrostatically with the amino groups of the surface. The payload delivery was triggered proportionally as pH lowered from 0% at pH 7.4 to 98% at pH 3.9. The authors also found that glutathione induced a change in the enzyme conformation with subsequent cargo release. These nanoparticles were tested in yeast cells, and cell death was induced when treated simultaneously with DOX-loaded nanoparticles and glutathione.

Bein and co-workers prepared MSNs loaded with fluorescein and capped with enzyme carbonic anhydrase (CA), which was bound reversibly through its active centre to the aryl sulphonamide groups grafted onto the surface of nanoparticles.[25] The CA-capped MSNs showed a negligible release at pH 7.4, whereas marked fluorescein delivery was observed at an acidic (5.5) pH. The release mechanism was based on protonation of sulphonamide in an acidic medium, which caused enzyme detachment and the uncapping of pores. Additionally, the enzyme was modified with an unnatural amino acid that contained a norborene moiety, which allowed for the additional site-specific attachment of tetrazine-modified targeting ligands, such as folic acid and anandamide. The targeting capability of the folate-functionalized system was tested on KB cancer cells, whereas the anandamide-functionalized system was tested on neural stem cells and A431 cells. Furthermore, the release in HeLa cells from CA-capped nanoparticles loaded with DAPI was investigated. It suggested that delivery was due to acidification throughout the endosomal pathway to late endosomes. Finally, the CA-capped nanoparticles loaded with actinomycin D (AmD) were

prepared and tested in HeLa cells. These nanoparticles produced an intracellular AmD release and caused remarkable cell death.

2.2. Glucose triggered release

Glucose-responsive MSNs capped with glucose oxidase (GOx) were developed by Lu and co-workers.[26] The external silica surface of MSNs was functionalised with prop-2-yn-1-yl(3-(triethoxysilyl)propyl) carbamate. Then inhibitor D-(+)-glucosamine was grafted through a click chemistry reaction. Rhodamine B (Rh B) was loaded into pores and GOx was used as caps via the formation of a complex with the grafted inhibitor. In the presence of glucose, GOx was displaced from the nanoparticles and a proportional dye release was observed. Other tested monosaccharides (i.e., fructose, mannose and galactose) did not induce the payload release.

Another glucose-responsive system, which also used GOx, was developed by Villalonga, Martínez-Máñez and co-workers.[27a] In this case, MSNs were loaded with $Ru(bipy)_3^{2+}$, functionalised with benzimidazole groups and capped with GOx that had been previously modified with β-cyclodextrin (β-CD). The CDs groups in CD-GOx formed an inclusion complex with the propylbenzymidazole stalks on the surface of nanoparticles by capping pores. In the presence of glucose, the GOx catalysed oxidation of glucose to gluconic acid, which induced the protonation of the benzimidazole group, resulted in CD-GOx displacement and clear cargo delivery. The systems were proposed as a potential glucose probe. The system gave not only a linear response to glucose within the $1x10^{-2}$-$1x10^{-4}$ mol L^{-1} range, but also and a LOD of $1.5x10^{-4}$ mol L^{-1}. Other saccharides (i.e. mannose, fructose, galactose, maltose and saccharose) produced no delivery. The same authors utilised this gating system on pore-expanded MSNs for delivery of insulin in simulated blood plasma.[27b]

An insulin delivery system responsive to glucose was described by Shi and co-workers, which used enzyme GOx.[28] MSNs with a pore size of ca. 12 nm were synthesised and pores were loaded with insulin. Then the loaded nanoparticles were coated with poly(ethyleneimine) through electrostatic interactions with silanol moieties on the external surface. The amino moieties of the poly(ethyleneimine) layer were reacted with glutaraldehyde. Then enzymes GOx and catalase (CAT) were immobilised through the formation of imine bonds. Addition of glucose led to its oxidation to gluconic acid by GOx, a drop in the pH of the microenvironment and a subsequent increase in coating multilayer permeability, which induced insulin release. The CAT enzyme was used to eliminate the hydrogen peroxide produced in the GOx-mediated reaction.

Villalonga, Martínez-Máñez and co-workers prepared MSNs loaded with $Ru(bipy)_3^{2+}$, functionalised on the outer surface with phenyl boronic acid moieties, and capped with lactose-modified esterase.[29] The neoglycoenzyme was linked to the surface by the formation of cyclic boronic acid esters with (i) the naturally-occurring glycosylation chains of the esterase and (ii) the synthetically-introduced lactose residues in the enzyme. The delivery system exhibited a two-step controlled cargo release triggered by glucose and ethyl butyrate. Presence of glucose resulted in the release of ca. half the cargo by the disruption of lactose-boronic acid linkages due to glucose competition. Addition of ethyl butyrate, which was transformed into ethanol and butyric acid by esterase, induced a subsequent drop in pH and the acid-mediated hydrolysis of boronic acid esters, which finally induced complete enzyme detachment and a full payload delivery. Furthermore, the authors loaded nanoparticles with DOX, and the nanodevice was used to release DOX in HeLa cells in the presence of a mixture of D-glucose and ethyl butyrate.

A more complex Janus-type nanodevice was described also later by Villalonga, Martínez-Máñez and co-workers.[30] The support consisted on Janus-type nanoparticles with gold and mesoporous silica faces on opposite sides. The mesoporous silica face allowed for cargo loading and functionalization whereas the Au face allowed the immobilization of certain enzymes. In this case, the silica matrix was loaded with $Ru(bipy)_3^{2+}$ and capped by the formation of inclusion complexes between grafted benzimidazole moieties and β-CDs. The Au side was also functionalized with two enzymes (GOx and esterase). Either D-glucose or ethyl butyrate was converted, by the enzymatic system, into gluconic acid or butyric acid to induce a local drop in pH, the protonation of the benzimidazole groups, the rupture of the benzimidazole-β-CD interaction and a payload delivery. The same authors prepared another nanodevice that incorporated enzyme urease together with GOx and esterase. In this three-enzyme nanodevice, the payload delivery from the silica matrix was triggered by glucose and was stopped by adding urea. This stop in cargo delivery was due to the neutralisation of an acidic medium by ammonia produced through the uresase-catalysed reaction. The GOx- and esterase-containing Janus nanoparticles were loaded with DOX and were successfully tested for DOX delivery in HeLa cells upon exposure to glucose, ethyl butyrate, or a mixture of both compounds.

2.3. Other stimuli

Slowing, Trewyn and co-workers used gold nanoparticles (AuNPs) and luciferase as caps to prepare gated MSNs responsive to reducing agents.[31] The silica surface was first functionalised with thiol moieties and later with [methoxy(polyethylenoxy)propyl]trimethoxysilane to obtain a PEGylated surface. Thiol moieties were further linked to 3-(propyldisulfanyl)ethylamine by the formation of disulfide bonds. Nanoparticles were loaded with luciferin (luciferase substrate) and capped with AuNPs functionalised with carboxylic-terminated poly(ethylene glycol) (PEG) through the formation of amide bonds with amino groups on the surface of MSNs. Finally, enzyme luciferase was physisorbed on the PEGylated external surface of capped MSNs by electrostatic interactions. In the presence of DTT, disulphide bonds were broken and a luminescent response was observed due to the simultaneous release of substrate luciferin from pores and enzyme luciferase from the surface. The designed system was tested in HeLa cells, which confirmed luciferin delivery due to the intracellular reducing environment.

Villalonga and co-workers reported a new delivery system based on Janus-type nanoparticles with opposing Au and mesoporous silica faces in which the enzyme urease mediated the conversion of urea to ammonia and the consequent cargo delivery.[32] In particular, the gold face was functionalised with a thiol-modified urease enzyme. Previously, the mesoporous silica face was loaded with $Ru(bipy)_3^{2+}$ and functionalised on the external

surface with 3-(2-aminoethylamino)propyl trimethoxysilane than acted as a molecular gate. The gate was closed at pH 5.0 due to the protonation of polyamines. In the presence of urea, a clear delivery of the entrapped ruthenium complex took place. The opening mechanism was based on transforming urea into CO_2 and NH_3 by urease, which induced a rise in pH and the subsequent deprotonation of polyamines.

Wang and co-workers recently described MSNs loaded with Rh 6G or DOX, and capped with enzyme α-chymotrypsin A (CTRA), which were capable of cargo release in the presence of CTRA inhibitor phenylmethanesulfonyl fluoride (PMSF).[33] To prepare the final device, MSNs were functionalised with APTES, loaded with the corresponding cargo and finally capped with CTRA through electrostatic interactions between the negatively charged enzyme and the positively charged protonated amino groups onto the silica surface. Upon PMSF addition or pH acidification, CTRA underwent a conformational change that induced its detachment from the surface of nanoparticles, which resulted in cargo release. The authors also found that the nanoparticles loaded with DOX were capable of cargo delivery in yeast cells upon the addition of PMSF. Fluorophore propidium iodide, which is cell-membrane impermeable, was also used as a cargo to demonstrate successful intracellular delivery.

Using enzyme-inhibitor interactions, Martínez-Máñez and co-workers have very recently prepared acetylcholinesterase-capped nanoparticles capable of delivering Rh B selectively in the presence of nerve agent simulant diisopropyl fluorophosphate (DFP).[34] MSNs were loaded with Rh B and the external surface was functionalised with a pyridostigmine derivative. Pyridostigmine is a well-known acetylcholinesterase reversible inhibitor. Finally, pores were capped by the interaction between the acetylcholinesterase active-site and the anchored pyridostigmine derivative (see Figure 3). DFP is a stronger inhibitor than pyridostigmine and was able to displace acetylcholinesterase from the silica surface, which resulted in clear cargo delivery. The detection system responded selectively to DFP and better than other nerve agent simulants and organophosphorus derivatives.

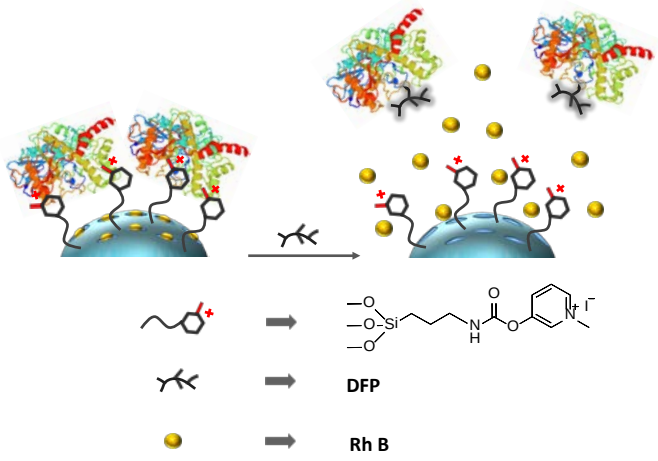

Figure 3. MSNs functionalised with a pyridostigmine derivative and capped with acetylcholinesterase enzyme. Pore opening and Rh B release was induced by presence of DFP.

pH-responsive capped MSNs were prepared by Yang and co-workers. MSNs were modified with poly(2-dimethylaminoethyl methacrylate) brushes by peroxidase mimetic catalytic atom transfer radical polymerization (ATRP) and loaded with rhodamine 6G.[35] PBS suspensions of the nanoparticles at pH 7.4 showed a moderate rhodamine 6G release. However, a marked dye delivery was observed upon lowering the solution pH to 2.0. The release was ascribed to electrostatic repulsions between positively-charged polymer chains that adopted an extended conformation with subsequent pore opening.

3. Enzymes as triggers

This section details gated MSNs capable of cargo release in the presence of enzymes. This approach offers an enormous potential by taking into account the vast number of gating ensembles that can be envisioned and can be hydrolysed/ modified by the presence of one enzyme or by a combination of enzymes. The examples in the next sections were classified after taking into account the type of enzyme used as a trigger.

3.1. Proteases and hydrolysis of amide groups

Avidin-biotin capped MSNs, for protease-responsive controlled releases, were prepared by Bein and co-workers.[36] MSNs were functionalised with propanethiol moieties and loaded with fluorescein. Then thiol groups were reacted with biotin-maleimide to yield a biotinylated surface. Pore closure was achieved upon avidin addition due to the formation of avidin-biotin complexes onto the surface of MSNs. Pore opening was achieved by adding protease trypsin. This protease hydrolysed avidin with the subsequent release of the entrapped fluorescein.

Another example of enzyme-responsive systems based on peptide-modified mesoporous silica was described by Heise *et al.*[37] In this work, silica microparticles functionalised with amines were loaded with fluorescein isothiocyanate (FITC)-functionalised dextran (4 kDa). A bioactive peptide shell, which consisted of Fmoc-terminated glutamic acid and enzyme-cleavable Ala-Ala bonds, was directly coupled to silica particles by stepwise Fmoc solid-phase peptide synthesis. The specific enzymatic hydrolysis of peptide linkers removed the bulky Fmoc groups and allowed the selective release of previously entrapped guest molecules.

Polymer-coated MSNs loaded with DOX and responsive to proteases were prepared by Bathia and co-workers.[38] Nanoparticles were first modified with *N*-(3-aminopropyl) methacrylamide hydrochloride (APMA), which bound MSNs electrostatically, and were loaded with DOX. Moreover, poly(ethylene glycol) diacrylate (PEGDA) was functionalised either with CGPQGIWGQGCR (highly degradable by MMPs) or CGPQGPAGQGCR (low degradable by MMPs) bis-cysteine peptides by a Michael addition reaction. Finally, a radical co-polymerisation between the acrylamide group of APMA and the terminal acrylate group of PEGDA-peptide yielded the coated material. Nanoparticles were incubated with 3T3-J2 fibroblasts and induced apoptosis was achieved due to DOX release as a result of the polymeric coating hydrolysis.

Deflavined GOx was used as a cap to prepare protease-triggered nanomaterials by Ren and co-workers.[39] MSNs were functionalised

with APTES and further reacted with glutaraldehyde. Then cofactor flavin adenine dinucleotide (FAD) was reacted with the aldehyde groups on the surface of MSNs by reductive amination. Nanoparticles were loaded with Rh B and capped with enzyme deflavined GOx, which was immobilised through the specific interaction with the cofactor. In the presence of protease K, GOx was digested with the subsequent Rh B delivery. The authors also demonstrated that no release of Rh B took place in the presence of protease K inhibitors, such as phenylmethyl-sulfonylfluoride and Hg^{2+}.

Martínez-Máñez and co-workers prepared MSNs loaded with DOX and capped with a cyclic peptide to obtain a nanomaterial to target B-cell non-Hodking's lymphoma (B-NHL), the most frequent malignant lymphoid neoplasm.[40] MSNs were loaded with DOX and the external surface of nanoparticles was decorated with alkyne moieties using a propargylamine derivative. Finally, pores were capped with an azide-functionalised T22 peptide analogue (that recognises the CXCR4 receptor in B-NHL cells) using a "click" chemistry reaction. Capped nanoparticles exhibited remarkable DOX release in the presence of proteases, whereas poor cargo delivery was observed when they were absent. Experiments in B-NHL cells allowed to assess the targeting effect of capped nanoparticles on CXCR4 receptor by flow cytometry. Finally, cytotoxic studies revealed a marked reduction in cell viability in B-NHL cells incubated with DOX-loaded nanoparticles.

A protease-responsive system loaded with two cytotoxic agents was reported by Van Rijt and co-workers.[41] The system consisted in MSNs loaded with non-toxic doss of cisplatin and bortezomib (Bz), functionalised with a specific biotin-heptapeptide (RSWMGLP) linker, which can be cleaved by MMP-9 and capped with avidin. The authors prepared MSNs that contained amino groups on the silica surface. Then the peptide linked to biotin was anchored to MSNs by the formation of amide bonds between the peptide carboxylic group and the amide moieties on the silica surface. Afterwards, nanoparticles were loaded with cisplatin and Bz, and were capped with avidin given its strong affinity to biotin. In the presence of MMP-9, the heptapeptide sequence was cleaved and nanoparticles exhibited remarkable cargo release. For the *in vitro* studies, A549 and H1299 (lung cancer) cells were transfected to overexpress MMP-9 and were treated with the nanoparticles. The authors demonstrated that a larger number of cells underwent apoptosis when treated with the solid loaded with both cytotoxics than when treated with the nanoparticles loaded with only one compound. Moreover, the therapeutic effect of nanoparticles on *Kras* mutant mice and the *ex vivo* tissue cultures from healthy and tumoural human lungs were also studied.

Martínez-Máñez and co-workers prepared pronase-responsive MSNs loaded with Rh B or DOX, and functionalised with polymer polyglutamic-acid, which acted as a capping unit.[42] In this case, polyglutamic-acid was anchored to the surface of MSNs previously modified with APTES thanks to the formation of amide bonds. In the presence of pronase, peptide bonds were cleaved and remarkable cargo release was observed. Capped nanoparticles were successfully tested in SK-BR-3 breast cancer cells.

In another work, the same research group also developed peptide-capped MSNs capable of releasing an entrapped cargo in the presence of protease enzymes.[43] For this purpose, MSNs were loaded with $Ru(bipy)_3^{2+}$ dye and the external surface was functionalised with azidopropyl moieties. Then pores were capped with 4-pentynoic acid-functionalised H-GGD EVD GGD EVD GGD EVD-OH peptide through a click chemistry reaction. The release of the entrapped complex was hindered in the absence of protease. However, when proteolytic enzymes from *Streptomyces griseus* (PESG) were present in the suspension, a marked payload release took place due to peptide hydrolysis (see Figure 4A).

The same authors also designed cathepsin B-responsive capped MSNs.[44] For this purpose, safranin O or DOX was loaded into the pores of MSNs and the external surface was functionalised with 3-(azidopropyl) triethoxysilane. A click reaction between the azidopropyl groups on the surface and an alkynyl-derivatised peptide (alkynyl-GIV RAK EAE GIV RAK-OH) was used to prepare the final capped nanoparticles (see Figure 4B). Studies have demonstrated that cargo release was achieved only in the presence of lysosomal extracts that contained cathepsin B. Moreover, the capped nanoparticles loaded with safranin O or cytotoxic drug DOX were also tested in HeLa cancer cells and primary culture cells of mouse embryonic fibroblasts (with cathepsin B overexpression). The authors found that safranin release in these cells was achieved through the action of cathepsin B. In fact preincubating cells with a cathepsin B-inhibitor remarkably reduced the safranin O-associated signal inside cells. Cell death was clearly observed when using the gated nanoparticles loaded with DOX. Also in this case, preincubating cell cultures with a cathepsin B inhibitor diminished cell death.

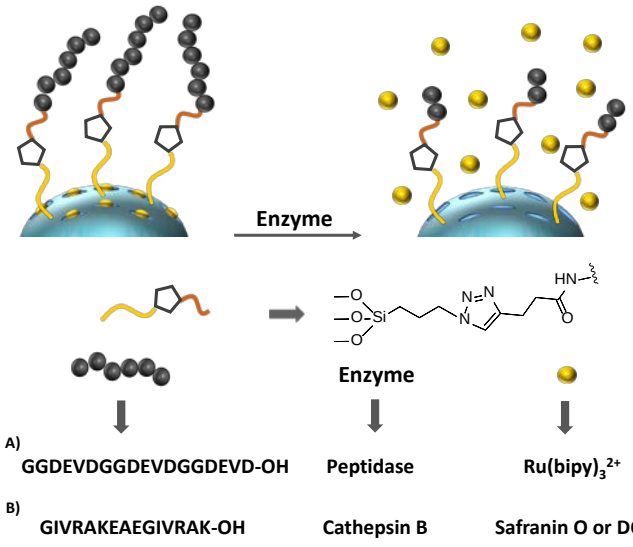

Figure 4. Controlled cargo release induced by peptidase or cathepsin B from MSNs capped with specific peptide sequences.

Li and co-workers also described cathepsin B-responsive capped nanodevices[45] using quantum dots (QDs) coated with a mesoporous silica shell. This silica shell was loaded with DOX and the surface was functionalised with aminopropyl moieties that were further reacted with a maleimide-PEG2-succinimidyl ester cross-linker. Afterwards, peptide CRRRQRRKKR-PGFK-EEEEEE was anchored to the silica surface by the formation of amide bond between the amine groups of the peptide and cross-linker. The peptide

contained the PGFK fragment, which is selectively hydrolysed by cathepsin B protease. The authors noted negligible DOX release when capped nanoparticles were suspended in PBS at pH 5.5. However, presence of cathepsin B induced remarkable DOX delivery. Further studies carried out with the peptide-capped nanoparticles showed remarkable DOX delivery in A549 cells (with high levels of cathepsin B) and negligible delivery in NIH 3T3 cells (with no cathepsin B activity). Moreover, A2780 (normal) and A2780Adr (DOX-resistant cells) were treated with either free DOX or nanoparticles. Free DOX could only reach the nucleus of A2780, whereas DOX was released in the nucleus of both cell lines when nanoparticles were used.

Feng He and co-workers reported MSNs loaded with DOX and capped with α-CDs, and an oligopeptide that was hydrolysed by enzyme cathepsin B.[46] The mesoporous support was functionalised with α-(2-aminoethyl)-aminopropyl trimethoxysilane, and the primary amino groups were further reacted with propargyl bromide to yield MSNs functionalised with stalks that contained alkyne and secondary amino moieties. In a second step, the pores of alkyne-functionalised MSNs were loaded with DOX and an inclusion complex between the secondary amino groups in the stalk, and α-CD was formed. Finally, a click reaction between alkyne moieties and a previously prepared azido-containing peptide GFLGR7RGDS prevented the dethreading of α-CDs. The PBS suspensions of capped nanoparticles (at pH 7.4 or 5.0) showed less than 10% DOX release (after 60 h) in the absence of cathepsin B. However in the presence of enzyme, a marked payload delivery was observed (ca. 80% at pH 5 and 70% at pH 7.4). Nanoparticles were more quickly internalised in HeLa (cancer) than COS7 (normal) cells, and the cytotoxic effect was higher in Hela cells.

Raichur and co-workers developed a trypsin-driven drug delivery system.[47] For this purpose, MSNs were loaded with diclofenac and the external surface of nanoparticles was functionalised with aminopropyl moieties. In a second step, protamine was grafted onto the external surface through the formation of imine bonds, using glutaraldehyde as a cross-linker. Minimal cargo release was observed in the absence of trypsin. However, selective diclofenac delivery was observed in the presence of the enzyme. These authors also evaluated the ability of capped MSNs to deliver anticancer drugs to colorectal cancer cells. For this purpose, MSNs loaded with the antineoplasic drug curcumin, and capped with protamine, were prepared. COLO205 cells were able to internalise protamine-capped nanoparticles and, as a result of the hydrolysis of the cap, intense curcumin fluorescence was observed inside cells. However, negligible curcumin fluorescence was observed when cells were incubated with curcumin suspended in water. Besides, cytotoxic studies also demonstrated that curcumin-loaded capped MSNs significantly enhanced anticancer activity compared with the free drug.

MSNs loaded with DOX and capable of cargo delivery in the presence of metalloproteinase (MMP) were developed by Zhang and co-workers.[48] As a first step, mercaptopropyl moieties were anchored onto MSNs and the thiol group was further reacted with S-(2-aminoethylthio)-2-thiopyridine, which resulted in the formation of disulphide bonds. DOX was loaded into mesopores and the amino moieties grafted onto the external surface were functionalised with propargyl bromide. Then a "click" chemistry reaction between the external alkyne moieties and mono-6-azido-β-CD was run. Afterwards, the N_3-GPLGVRGRGDK-adamantane peptide was used to form inclusion complexes with the β-CD onto the nanoparticle surface. In the last step, the azide group of the peptide was reacted with alkyne-modified poly(aspartic acid) polymer to yield the final material. Fragment PLGVR can be recognised and triggered by MMP. The controlled release behaviour of the prepared solid was evaluated *in vitro* using the SCC-7 (squamous carcinoma) and HT-29 (human colon cancer) cell lines, which overexpress MMP, and with non-cancerous cells 293T (human embryonic kidney) as controls. These studies demonstrated that the capped MSNs loaded with DOX were internalised by cells. The hydrolysis of the PLGVR fragment by MMPs in tumoural cells, led to DOX being delivered and induced SCC-7 and HT-29 cell apoptosis.

MMP-9 enzyme-responsive nanoparticles were prepared by Wang and co-workers.[49] The pores of MSNs were loaded with DOX and the external surface was functionalised with aminopropyl moieties. In a second step, external amino groups were reacted with glutaraldehyde and pores were capped upon gelatine addition. Aqueous suspensions of the capped nanoparticles at pH 7.4 showed negligible drug release, whereas moderate delivery was noted in the presence of MMP-9. Release of DOX was ascribed to the hydrolysis of gelatine coating by enzyme MMP-9. The intracellular uptake and cytotoxicity of the gelatine-capped nanoparticles were studied using the LO2 (with no MMP-9 activity) and cancer HT-29 (with MMP-9 activity) cell lines, which evidenced an efficient response only in the cancer HT-29 cells. *In vivo* studies in xenograft mice models (HT-29) showed delayed tumour growth upon the injection of DOX-loaded gelatin-capped nanoparticles.

Cai and co-workers synthesised peptide-capped MSNs responsive to MMPs.[50] MSNs were functionalised with APTES, and then the carboxylic groups of a modified peptide sequence (Fmoc-$NH(CH_2)_5CO$-PLGLARR-$(CH_2)_5COOH$) were attached to the amino groups on the silica surface through the formation of amide bonds. Nanoparticles were loaded with DOX and the peptide was linked by its free end to bovine serum albumin (BSA) to cap pores. Finally, lactobionic acid (LA) was covalently attached to BSA in order to achieve better cell targeting and to improve endocytosis efficiency; 58% of DOX was released in the presence of MMP-13 after 8 h, while only 18% was delivered when the enzyme was absent. The authors observed that nanoparticles had a cytotoxic effect on HepG2 cells. *In vivo* studies were performed in mice injected with HepG2 cells to obtain the tumour model. Reduced tumour weight and volume were observed in the mice treated with nanoparticles.

Following this idea, the same group designed MSNs functionalised with an MMP-2-sensitive peptide and capped with phenylboronic acid (PBA)-conjugated human serum albumin (HAS).[51] In order to prepare the final material, MSNs were modified with 3-(triethoxysilyl)propyl succinic anhydride, which was hydrolysed to yield MSNs functionalised with carboxylic groups. MSNs were further reacted with a specific polypeptide (NH_2-GR_9PVGLIGG-COOH) and loaded with DOX. Finally, nanoparticles were capped by a reaction between the amino groups of the previously obtained PBA-HAS complex and the carboxylic groups at the end of the polypeptide on the silica surface. The delivery studies showed that DOX release was negligible when there was no enzyme

in the medium, whereas remarkable delivery was observed in the presence of MMP-2 due to the hydrolysis of the PVGLIG sequence in the peptide. The authors used three different cell lines (HepG2, L-7702 and Raw264.7) to carry out *in vitro* studies, and they centred the cytotoxicity assays on HepG2 to accomplish good inhibition of cell growth when the DOX-loaded MSNs were in cultured media. For the *in vivo* studies, mice were injected with different treatments (blank, free DOX or nanoparticles). For the HepG2 xenografted mice treated with the DOX-loaded MSNs, the volume and weight of tumours lowered and side-effects diminish compared to free DOX.

Zhang and co-workers prepared a therasnostic system based on CPT-loaded peptide-capped MSNs responsive to MMP-2.[52] The authors synthesised a specific peptide (GPLGVRGKK-N_3) with a terminal azide group. This peptide was functionalised with quencher 4,4-dimetylamino-azobenzene-4'-carboxylic acid (Dabcyl), which was coupled to the primary amine of lysine and with dye carboxytetramethylrhodamine hydrochloride (TAMRA), which was coupled to the *N*-terminal of the peptide. MSNs were functionalised with alkyne groups and loaded with CPT. Then the peptide derivative and an additional tumour targeting peptide (RGDFK-N_3) were attached by a "click" reaction. In the absence of MMP-2, the system was capped and the proximity between TAMRA and Dabcyl resulted in no fluorescence. In the presence of MMP-2, the capping peptide was cleaved, TAMRA fluorescence was activated (due to the separation from the quencher) and CPT was released. The therasnostic system was tested in SCC-7 cancer cells with high MMP-2 expression and in COS7 normal cells that did not overexpress this enzyme. It was demonstrated that CPT was selectively released in cancer cells and that endocytosis was enhanced due to the interactions between the targeting peptide and cell receptors.

Martínez-Máñez and co-workers used ε-poly-L-lysine as caps to prepare amidase-responsive nanoparticles.[53] MSNs were loaded with $Ru(bipy)_3^{2+}$ and the external surface was functionalised with ε-poly-L-lysine by two different strategies; i.e. (i) the random formation of urea bonds between isocyanate-functionalised MSNs and the amino groups located on the ε-poly-L-lysine backbone and (ii) the reaction between an alkyne derivative of ε-poly-L-lysine with azidopropyl-functionalised MSNs. In both cases, selective cargo delivery in the presence of amidase was observed due to the amide bond hydrolysis of the peptide. Cell internalisation and $Ru(bipy)_3^{2+}$ delivery studies were carried out with both gated materials in HeLa cells. Furthermore, HeLa cell treatment with the ε-poly-L-lysine-capped nanoparticles loaded with cytotoxic drug camptothecin (CPT) efficiently reduced cell viability.

Amidase and pronase responsive MSNs were developed by the research group of Martínez-Máñez.[54] MSNs were loaded with safranin O and treated with excess *N*-(3-triethoxysilylpropyl)gluconamide to obtain a dense polymeric gluconamide layer to coat nanoparticles. In the presence of amidase or pronase, gluconamide moieties were hydrolysed with subsequent pore uncapping and safranin O release. The authors also found that nanoparticles successfully delivered the cytotoxic drug CPT in the HeLa and MCF-7 cancer cells due to the degradation of the molecular gate by lysosomal enzymes. The same authors reported MSNs capped with a bulky molecule that contained amide and urea moieties. The mesoporous support was loaded with $Ru(bipy)_3^{2+}$ and a molecule that contained amide and urea bonds at predefined positions was anchored to the external surface as a cap.[55] In the presence of amidase, 40% of the dye was released due to the hydrolysis of the amide bonds at the far end of the capping molecule. In the presence of urease, the hydrolysis of the urea bond near the silica surface resulted in a more drastic uncapping of pores and 80% of the cargo was delivered. A synergistic effect was observed in the presence of both enzymes, which resulted in fast complete cargo delivery. Furthermore, these nanoparticles were internalised by HeLa and MCF-7 cell lines, and they successfully delivered their cargo in the lysosomal compartment. The capped nanoparticles loaded with CPT were also prepared and were able to induce HeLa cell death.

A pancreatin-responsive material loaded with pro-drug sulfasalazine (SZ) was reported by Yu and co-workers.[56] Firstly, MCM-48-type nanoparticles were functionalised with APTES and then loaded with SZ. In order to cap the pores of nanoparticles, succinylated soya protein isolate (SSPI) was anchored to the external surface by the formation of amide bonds. A payload release was studied under different gastrointestinal simulated conditions: (i) stomach (pH 1.2, in the presence of pepsin, 2 h), duodenum (pH 5.5, 1 h) and the small intestine (pH 7.4 in the presence of pancreatin, > 8 h). Whereas no release was observed in the simulated stomach and duodenum, prodrug SZ was released in the simulated small intestine due to the hydrolysis of the SSPI cap induced by pancreatin. The authors also demonstrated that in the presence of azo-reductase producing bacteria, which are present in the lower part of the small intestine and colon, SZ was converted into its active metabolite 5-aminosalycilic acid.

Martínez-Máñez and co-workers reported thrombin-responsive MSNs, which were loaded with acenocoumarol (an anticoagulant drug) or safranin, and were capped with a specially designed peptide (LVPRGSGGLVPRGSGGLVPRGSK) that contained three repeats of the thrombin cleavage site.[57] The peptide contained a pentinoic acid at one end, which was used to attach the sequence to the previously azide-functionalised silica surface via a copper(I)-catalysed click reaction. In the presence of thrombin, the specific peptide was hydrolysed and resulted in cargo release. Acenocoumarol-loaded MSNs were proven to prolong the coagulation time of blood plasma in the presence of thrombin.

Martínez-Máñez and co-workers prepared peptide-capped MSNs loaded with safranin for cargo delivery, triggered by caspase 3 (C3).[58] The peptide (KKGDEVDKKARDEVDK) contained two repeat units of a target sequence (DEVD), known to be hydrolysed by C3. MSNs were functionalised with 3-(azidopropyl) triethoxysilane, loaded with safranin and then the alkyne-containing peptide sequence was attached by a click reaction to the azide groups on the silica surface. In the absence of C3, the system showed minor release, whereas remarkable payload delivery was observed in the presence of the enzyme due to the hydrolysis of the peptide sequence. The prepared MSNs were internalised in HeLa cells by electroporation to avoid endocytosis by taking into account the cytoplasmatic location of C3. In order to induce C3, cells were treated with staurosporin (STS), which resulted in apoptosis with the consequent C3 activation in the cytosol. Safranin delivery in cells was observed only when C3 was activated. The sequence of a cell-penetrating peptide was added to the *N*-terminal end of the

capping peptide and was used to prepare an additional solid, which was able to internalise and deliver its payload in C3-activated HeLa cells without requiring electroporation.

3.2. Hydrolysis of ester and phosphodiester groups

Esterases have been extensively used as triggers by taking into account the fact that they are enzymes capable of hydrolysing the ubiquitous ester linkage. The first esterase-driven gated MSN was published by Stoddart and co-workers. These authors loaded MSNs with Rh B and the external surface was functionalised with PEG stalks that encircled α-CDs and finished with an ester-linked adamantly bulky stopper (see Figure 5A). In the presence of porcine liver esterase (PLE), the ester linkage was hydrolysed with the subsequent removal of adamantly stopper, which resulted in Rh B release.[59,60] The same authors prepared a closely related system, but by loading MSNs with fluorescein or CPT, and then capping pores with the PEG stalks encircled with α-CDs, which ended with folic acid (FA) as a stopper (see Figure 5B). Once again, addition of PLE induced cargo release. The gated nanoparticles loaded with CPT were efficiently endocyted by human osteosarcoma U2Os cells and induced marked cell death, which was more marked than that obtained with the cells treated with the free drug.[61]

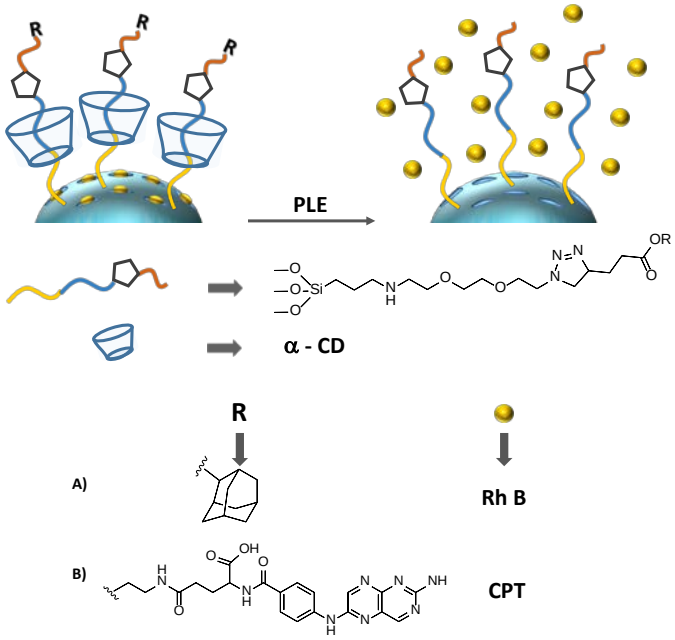

Figure 5. PLE-induced controlled release of A) Rh B and B) CPT from the MSNs capped with and A) the ester-linked adamantyl stopper or B) with an ester-linked FA stopper.

Some of us have reported a gated material composed of MSNs loaded with the $Ru(bipy)_3^{2+}$ complex and capped with oligoethyleneglycol chains that contain an ester linkage. Water suspensions of nanoparticles at pH 8.0 showed negligible cargo release due to the presence of bulky oligoethyleneglycol chains around pore outlets. In the presence of esterase, marked dye delivery was observed due to ester linkage hydrolysis and the detachment of bulky oligoethyleneglycol chains.[62] The esterase-induced opening mechanism was corroborated because amidase, urease and denaturated esterase were unable to induce pore opening. Besides the nanoparticles loaded with CPT were internalised by HeLa cells, which triggered cell death due to the hydrolysis of capping ester-containing glycol chains in lysosomes and drug release. In another work, the same authors prepared MSNs loaded with Rh B, with the external surface functionalised with polyester polymers that contained side-chain azobenzene moieties.[63] In the absence of the esterase enzyme, negligible dye release was observed, whereas a marked payload delivery took place in the presence of the enzyme. CPT-loaded capped nanoparticles induced cell death in HeLa cells.

[2]Pseudorotaxanes derivatives were used as esterase-hydrolysable caps by Yang and co-workers.[64] For this purpose, the authors synthesised a carboxylic acid-choline derivative. This derivative was anchored to the silanol groups on the surface of MSNs through an esterification reaction. Then the functionalised material was loaded with Rh B and capped by the formation of [2]pseudorotaxanes between the grafted choline derivative and *p*-sulfonato-calix[4]arene. The PBS suspensions of the capped nanoparticles showed negligible Rh B release in the absence of esterase, but remarkable cargo delivery in the presence of the enzyme. Cargo release was ascribed to the hydrolysis of the ester linkage that resulted in the dethreading of [2]pseudorotaxane from the surface. Addition of ethanediamine to suspensions of nanoparticles induced pore opening and Rh B delivery due to the competitive binding of this molecule with *p*-sulfonato-calix[4]arene.

Polycaprolactone (PCL) was used as a capping agent to develop esterase-triggered nanodevices by Gooding and co-workers. These authors used pore-expanded MSNs as an inorganic support, which was loaded Rh B or DOX. Then PCL was also loaded and the external surface was functionalised with aminopropyl moieties. Finally, nanoparticles were coated with polyacrylic acid (PAA) through electrostatic interactions with anchored protonated amines.[65] Cargo release was observed only at pH 5.5 and in the presence of esterase. At an acidic pH, the PAA layer was detached from the external surface to allow esterase to access the interior of pores with subsequent PCL hydrolysis and entrapped cargo release. The nanoparticles loaded with Rh B were internalised by HeLa, neuroblastoma (SK-N-BE(2)) and fibroblast (MRC-5) cells, with no reported cytotoxic effect. An 8-fold toxicity increase in SK-N-BE(2) cells was observed when nanoparticles where loaded with DOX.

PCL was also used by Zhou and co-workers to prepare esterase-triggered nanodevices that used MSNs with carbon quantum dots embedded in the silica matrix. MSNs were reacted with functionalised 3-(trimethoxysilyl)propyl methacrylate to yield alkene moieties on the silica surface. Afterwards, cysteamine and 2-(dimethylamino)ethanethiol (DME) were grafted on MSNs by thiolene "click chemistry". Next, a further reaction of 2,3-dimethylmaleic anhydride (DMA) with cysteamine yielded a zwitterionic surface (composed of oppositely-charged moieties; i.e. $-COO^-$ from DMA and $-NH^+(CH_3)_2$ from DME). The anionic part was designed to be protonated at a pH below 6.8. Finally, pores were loaded with DOX and closed upon the addition of PCL, which was physisorbed in pore outlets via an impregnation process.[66] At pH 6.8, the zwitterionic surface became positive due to the protonation of the carboxylic moieties and the esterase-triggered

DOX release. In the presence of esterase at a pH higher than 6.8, no release was noted due to the repulsion between the zwitteronic layer and the enzyme. Besides, the PLE-capped nanoparticles had a strong cytotoxic effect on SCC cancer cells due to their higher extracellular acidity (pH < 6.8), whereas DOX release in HaCaT (normal cells) was negligible due to the repulsion between the zwitteronic layer and the enzyme at a pH above 6.8.

The hydrolysis of phosphate esters has also been used as an opening mechanism in certain gated nanodevices. In these examples, acid phosphatase and DNAse I (which cleaves DNA preferentially at the phosphodiester linkages adjacent to a pyrimidine nucleotide) were used as triggers. In a first example, MSNs were loaded with $Ru(bipy)_3^{2+}$ and the external surface was functionalised with a linear triamine. The capped material was obtained after adding ATP, which formed supramolecular complexes with the positively-charged amino moieties on the surface.[67] In the absence of acid phosphatase, negligible dye release was observed. However in the presence of the enzyme, marked $Ru(bipy)_3^{2+}$ delivery was seen due to ATP hydrolysis. These capped nanoparticles were mixed in a second step with gelatine and glutaraldehyde to construct a 3D scaffold in which acid phosphatase-triggered delivery was assessed. Studies carried out with the human osteoblast cell line HOS showed that the scaffold did not elicit any cytotoxic effect, and that cells adhered, proliferated and spread well in the scaffold.

The first example of capped nanoparticles triggered by DNAse I was reported by Zhu and co-workers in 2011. These authors used hollow MSNs with pores loaded with fluorescein and the external surface functionalised with aminopropyl moieties.[68] Pores were finally capped upon the addition of a negatively-charged cytosine-phosphodiester-guanine oligodeoxynucleotide by a simple electrostatic interaction with the positively-charged protonated amino moieties onto the surface. In the absence of DNAse I, negligible fluorescein release was observed, whereas the cap was hydrolysed and cargo was delivered when it was present. Wu and co-workers followed a similar procedure and prepared MSNs loaded with colchicine and with the external surface also functionalised with aminopropyl groups. However in this case, the authors capped colchicine-loaded nanoparticles using several negatively-charged single-stranded DNAs of edible plants *Solanum lycopersicum* and *Triticum aestivum*.[69] Once again, cargo release was observed in the presence of DNAse I due to the hydrolysis of capping DNAs.

Willner and co-workers prepared four different functionalised MSNs with amino groups and linked DNA sequences by covalently using sulfo-EMCS.[70] The first nanodevice was loaded with Rh B and capped with a DNA sequence (DNA-1) capable of forming a hairpin at room temperature to block pores. The gate contained a single sequence strand, which can be recognised by a nucleic acid biomarker (i.e. 5'-AGT GTG CAA GGG CAG TGA AGA CTT GAT TGT-3'). When the biomarker was added to the suspension of nanoparticles, the hairpin opened and formed a duplex, but pores remained closed and no dye was released until the Exo III enzyme was added. This enzyme hydrolysed the 3'-end of the sequence and allowed the release of Rh B. Another sequence was grafted (DNA-2) and 5'-ATC CTC AGC TTC G-3' was used as a biomarker. The formed DNA duplex was able to cap pores and to maintain the cargo inside pores. Enzyme Nb.BbvCI produced the duplex dissociation due to the specific cleavage of one base, and cargo was released. The third nanodevice was functionalised with DNA-3, and also with a hairpin structure, and an ATP-aptamer conjugated with a sequence hydrolysable by enzyme Exo III was incorporated. The hairpin open upon the addition of ATP and enzyme Exo III, which hydrolysed the 3' end of DNA-3. For the last material, DNA-4 was grafted onto the surface. DNA-4 contained an ATP-aptamer and a sequence hydrolysable by enzyme Nb.BbvCI. The authors used DNA-3 capped material loaded with CPT for the cellular uptake studies in MDA-MB-231 (breast cancer cells) and MCF-10a (normal breast cells). After the endocytosis of nanoparticles, approximately 40% more cancer cells died compared with normal cells.

3.3. Glycosidic linkages

Glycosidases are present in almost all living organisms where they play diverse and different roles. Glycosidases catalyse the hydrolysis of glycosidic linkages by degrading oligosaccharides and glycoconjugates. The first example of a porous support gated with "saccharides" was published by Martínez-Máñez and co-workers.[71] Mesoporous silica microparticles were loaded with $Ru(bipy)_3^{2+}$ and capped with the trialcoxysilane-lactose derivative. Suspensions of this material were stirred in both the presence and absence of β-D-galactosidase enzyme, which induced progressive cargo release (see Figure 6A). In another work, the same authors used Glucidex 47, Gludicex 39 and Glucidex 29-trialkoxysilane derivatives (Glucidex is a hydrolysed starch) as molecular gates and $Ru(bipy)_3^{2+}$ as the cargo in a mesoporous silica support.[72] In the absence of pancreatin, cargo release was inhibited, while the hydrolysis of the glycosidic bonds and dye release occurred in the presence of this mix of amylase enzymes (see Figure 6B). HeLa and LLC-PK1 cells were incubated with $Ru(bipy)_3^{2+}$-loaded Glucidex 47-capped nanoparticles to study cellular uptake by confocal microscopy. Nanoparticles were internalised by endocytosis, and concentrated in endosomes and lysosomes. Cytotoxicity assays revealed that capped MSNs were biocompatible. The same Glucidex 47-capped nanoparticles, but loaded with DOX, were clearly toxic for HeLa cells. The microparticles loaded with garlic extract and capped with Glucidex 47 were also prepared by the same authors.[73] The capped material was embedded into a nylon-6 membrane and the release properties of the nanocomposite were tested in the presence of pancreatin, which hydrolysed starch and aimed cargo delivery.

In 2012, the same research group prepared silica nanoparticles with Rh B as the cargo, capped with the galacto-oligosaccharide (GOS)-trialcoxysilane derivative.[74] Suspensions of the capped nanoparticles showed negligible cargo release, whereas Rh B was delivered in the presence of β-galactosidase (see Figure 6C). Release experiments were performed in yeast cells, in which β-galactosidase was found at normal concentrations or was overexpressed. Rh B only stained cells that overexpressed the enzyme because of the hydrolysis of the capping GOS and cargo release. The same experiment was carried out with X-linked *Dyskeratosis congenita* (X-DC) patient´s fibroblast (β-galactosidase was overexpressed) and in H460 cells (β-galactosidase was not overexpressed). In the former cell line, Rh B delivery was much more significant.

Qu and co-workers prepared Rh B-loaded MSNs capped with Konjac oligosaccharide (KOGC), a derivate of Konjac plants.[75] The delivery behaviour of the solids capped with different quantities of KOGC in the presence of different enzymes was studied, and cargo delivery was observed only in the presence of β-mannanase, an enzyme secreted by bacteria that can hydrolyse KOGC (see Figure 6D). Internalisation and biocompatibility studies were performed by incubating Caco-2 cells with Rh B-loaded KOGC-capped MSNs. Nanoparticles were endocytosed by cells and cell viability was not affected.

Other polysaccharides have been used as molecular gates; e.g., Qu and co-workers loaded MSNs with Rh B, functionalised the external surface with APTES, and capped nanoparticles with hyaluronic acid (HA) using EDC (1-ethyl-3-(3-dimethylaminopropyl)carbodiimide hydrochloride) /*N*-hydroxysuccinimide (NHS).[76] Hyaluronidase (HAase) is an enzyme present in tumour environments that is capable of hydrolysing HA. Release experiments showed that the cargo was delivered only in the presence of HAase. Two cell lines, NIH3T3 and MDA-MB-231, were incubated with Rh B-loaded HA-capped MSNs, where internalisation was much higher in the MDA-MB-231 cells (which overexpress the CD44 receptor) and demonstrated the targeting effect of HA. The same nanoparticles loaded with DOX showed toxicity to MDA-MB-231 cells.

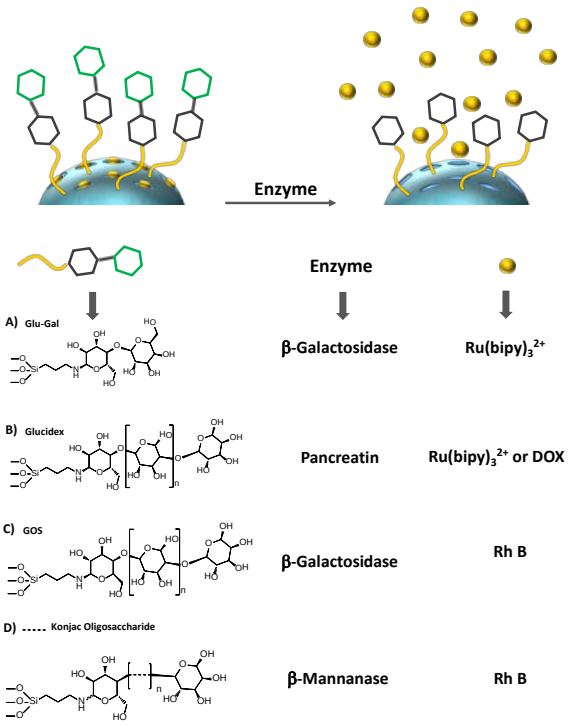

Figure 6. Controlled cargo release from saccharide-capped MSNs triggered by the hydrolysis of glycosidic bonds.

The same authors prepared up-converting nanoparticles (UCNPs, $NaGdF_4$:Yb,Tm), firstly coated with a silica shell and then with mesoporous TiO_2.[77] The TiO_2 shell pores were loaded with DOX and capped with HA by electrostatic interactions. Suspensions of capped nanoparticles in buffer at pH 4.3 showed only 17% of cargo release, whereas DOX release reached 95% in the presence of HAase. Both the NIH3T3 and MDA-MB-231 cell lines were incubated with capped nanoparticles, yet the emission intensity from $NaGdF_4$:Yb,Tm was observed only in cancer MDA-MB-231 cells (due to the interaction of HA with the overexpressed CD44 receptor on the membrane of these cells). These authors aimed to use gated nanoparticles in photodynamic therapy. For this purpose, they irradiated the $NaGdF_4$:Yb,Tm core with 980 nm light by inducing an energy transfer process, which activates TiO_2 to produce ROS. The nanoparticles activated with NIR light caused more cellular death than with only the effect of DOX released from the nanodevice. This fact was ascribed to the combination of both NIR light and HAase stimuli, which simultaneously induced ROS generation and DOX release.

Another example of HA-capped material was described by the same authors. They loaded DOX in gold nanocrystals (AuNCs) of 50 nm that contained pores between 5 nm and 8 nm, and capped them with dopamine-derivatised HA.[78] HA was functionalised with dopamine (DA) by a condensation reaction using EDC/NHS. The amino groups in DA-HA interacted with the surface of AuNCs and capped pores. DOX delivery was induced by HAase and improved with NIR light. The same above-mentioned assays with MDA-MB-231 cells were performed, and the authors demonstrated the nanodevice's effectiveness. Nanoparticles were internalised by MDA-MB-231 cells through HA-CD44 interactions, and the cumulative effect of released DOX and NIR irradiation reduced cell viability to only 18%. Besides, nude mice xenografted with MDA-MB-231 cells were treated intratumourally with both DOX-loaded HA-capped AuNCs and NIR irradiation, which induced subsequent tumour ablation.

Wang and co-workers prepared a mesoporous silica-based system that was sensitive to both redox and enzyme stimuli, and capable of targeting receptor CD44 in cells.[79] MSNs were functionalised with (3-mercaptopropyl) trimethoxysilane and pores were loaded with DOX. The thiol groups on the surface were conjugated with S-(2-aminoethylthio)-2-thiopyridine. Finally, pores were capped with HA through the formation of amide bonds. The kinetics studies carried out with HA-capped MSNs revealed that when nanoparticles were suspended in PBS at pH 5.0 in the presence of GSH and HAase, 60% DOX was released. However when both stimuli were absent, only 20% of DOX was delivered. The authors studied the internalisation of HA-capped MSNs in HCT-116 (which overexpress the CD44 receptor) and NIH-3T3 (as a negative control) cells. HA-capped MSNs were more efficiently uptaken by HCT-116 than by NIH-3T3 cells. Cytotoxicity assays revealed that the IC_{50} of HA-capped MSNs for HCT-116 cells was 0.6 μg mL^{-1}, but was 4.5 μg mL^{-1} for NIH-3T3.

Qu and co-workers prepared Fe_3O_4 magnetic nanoparticles coated with a mesoporous silica shell and loaded with DOX or chlorambucil (Chl). HA was functionalised with double bonds by reacting HA with methacrylic anhydride to obtain a methacrylated hyaluronic acid (m-HA) polymer. The external silica surface was functionalised with APTES and covered (through electrostatic interactions) with m-HA.[80] Drug release studies were carried out by suspending nanoparticles in PBS buffer solution at pH 7.4 without HAase to simulate normal tissue, or in PBS solution at pH 5.0 with HAase to simulate a tumour environment. The nanoparticle

suspension at pH 7.4 in the absence of HAase showed negligible DOX release (less than 10% after 24 h), but marked release was observed (50% after 24 h) at pH 5.0 and in the presence of the enzyme. Chl released from nanoparticles reached 30% (after 24 h) at pH 7.4 in the absence of HAase, whereas the release was 100% after 24 h at pH 5.0 and in the presence of the enzyme. Cellular uptake and delivery studies in the HeLa and MDA-MB-231 cell lines were carried out with the prepared materials. Cytotoxicity studies in cancer cells (HeLa and MDA-MB-23) and in normal cells (L02 human hepatocytes and HUVEC) indicated that coated nanoparticles showed weak toxicity to normal cells, but strong toxicity to tumour cells.

Chen and Liu prepared fluorescein-labelled MSNs capped with HA and capable of entrapped cargo release in the presence of HAase.[81] MSNs were functionalised with APTES and nanoparticles were further labelled by reacting fluorescein isothiocyanate with the amino groups on the silica surface. Nanoparticles were loaded with DOX and finally capped with HA via electrostatic interactions between the carboxylic groups in HA and the protonated amines on the surface of MSNs. At a slightly acidic pH (6.8), which simulated fluid in tumour tissue, capped MSNs formed hydrogels of ca. 10,000 nm due to the hydrogen bond interactions between the carboxyl groups from HA from several nanoparticles. Cargo release from hydrogels at pH 6.8 was studied in the absence and presence of HAase. No release occurred in the absence of the enzyme, but remarkable cargo delivery was observed due to the hydrolysis of HA in the presence of HAase. Nanoparticles were tested in both human breast cancer cells (SKBR3) and human embryonic kindness cells (293T). DOX was delivered preferentially in cancer cells due to the presence HAase and the high expression of CD44 antigen, which is a receptor for HA.

Chitosan has also been used as molecular gates to design enzyme-responsive capped materials. For example, Lou and co-workers functionalised mesoporous silica with APTES and made it react with succinic anhydride. The material was loaded with Rh B or DOX, and capped with chitosan by amide formation using EDC/NHS.[82] Cargo release was observed either in the presence of lysozyme at pH 7 or by changes in pH, particularly at pH 4.

Kim and co-workers reported α-amylase and lipase-responsive MSNs, which were capped with β-CDs and loaded with calcein.[83] MSNs were functionalised with APTES, which were later reacted with propargyl bromide to yield alkyne groups on the silica surface. Then nanoparticles were loaded with calcein and capped with mono-6-azido-β-CDs by a click chemistry reaction. A second solid was capped using β-CDs linked to the silica through an o-nitrobenzyl ester moiety on the stalk part. For this second solid, firstly an *o*-nitrobenzyl ester derivative was linked to amino-functionalised MSNs by an amide bond and then mono-6-azido-β-CD was attached to the ester by a click reaction. Both solids showed remarkable cargo release in the presence of α-amylase due to the hydrolysis of β-CD. The solid that contained o-nitrobenzyl ester moiety was able to deliver the cargo in the presence of lipase. When both α-amylase and UV were used as stimuli, calcein release from the second solid accelerated since o-nitrobenzyl ester is a photocleavable linker.

By employing pancreatin enzyme as a stimulus, Martínez-Máñez and co-workers developed the first example of a family of gated nanoparticles that communicate by exchanging chemical messengers.[84] The communicating system consisted of three different solids. In the presence of pancreatin, the first solid delivered a chemical messenger, which was able to open the second type of nanoparticles. This delivered another messenger that opened a third gated material. The first solid was loaded with reducer tris(2-carboxyethyl)phosphine (TCEP) and was capped with a galacto-oligosaccharide (GOS)-trialcoxysilane derivative, as in Reference 74. The second MSNs were loaded with dodecyltrimethylammonium bromide (DTAB) and capped with a PEG linked to the silica surface through disulphide bonds (sensitive to TCEP). Finally for the third solid, MSNs were loaded with safranin-O and capped with a lipid bilayer (prepared from 1,2-dioleoyl-sn-glycero-3-phosphocholine, DOPC), which was disrupted in the presence of DTAB.

Lou, Xia and co-workers prepared DOX-loaded MSNs capped with cellulose for controlled drug delivery triggered by enzyme cellulase glycosidase and pH.[85] The external surface of MSNs were functionalised with carboxylic groups and pores were loaded with DOX. Cellulose was attached to nanoparticles through ester linkages between the COOH groups on the silica surface and the OH groups in the biopolymer. Negligible release was observed at pH 7.4, yet DOX delivery increased at an acidic pH due to the hydrolysis of ester linkages and the uncapping of pores. Pore opening and DOX delivery were observed in the presence of cellulose glycosidase at pH 7.4 due to the rupture of the glycoside bonds of the biopolymer. The authors prepared the same nanoparticles labelled with fluorescein, which were successfully tested for intracellular DOX delivery in HepG2 tumour cells.

3.4. Rupture of azo bonds

Reductases are enzymes present in intestinal microflora and capable of reducing azo bonds. Martínez-Máñez and co-workers prepared MSNs loaded with Rh B or CPT, and capped with a bulky azopyridine derivative (Figure 7A).[86] The authors demonstrated that cargo delivery from gated-MSNs only occurred in the presence of reductase or esterase enzymes, whereas the nanodevice remained capped with pepsin (an enzyme present in stomach). The authors suggested that nanoparticles could be used as a specific drug delivery system in colonic diseases. Moreover, HeLa cells treated with CPT-loaded nanoparticles underwent apoptosis due to nanoparticle internalisation and pore opening.

With a similar approach, Sun and co-workers loaded MSNs with IBU and functionalised the external surface with APTES. The reaction between the amino groups on the surface of nanoparticles and azobenzene-4,4′-dicarboxylic acid yielded the final capped system.[87] Negligible IBU release took place when capped nanoparticles were suspended in simulated gastric fluid (SGF) for 1 h or in simulated intestinal fluid (SIF) for 4 h (see Figure 7B). However when capped nanoparticles were suspended in simulated colonic fluid (SCF), IBU release rose to more than 83%. This marked IBU release was ascribed to the hydrolysis of the azo bond by reductases and subsequent pore opening.

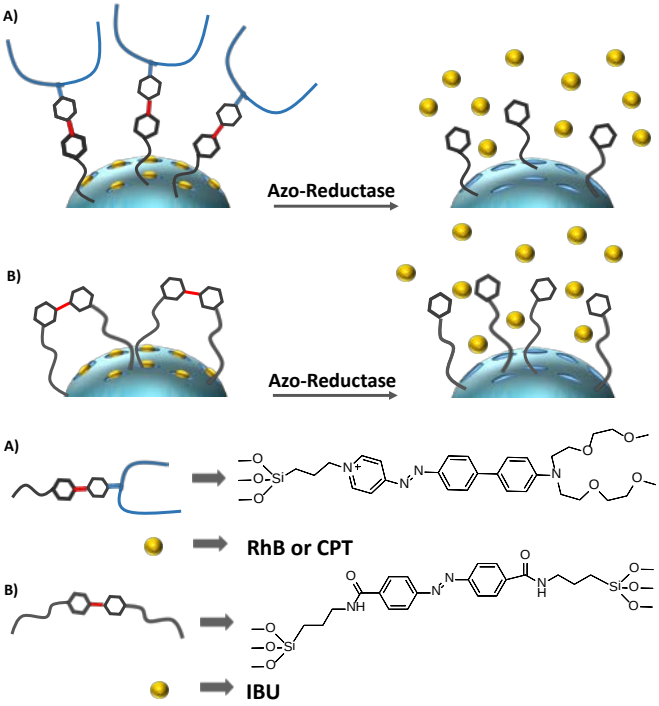

Figure 7. Reductase-induced controlled cargo release from MSNs functionalised with azo derivatives.

3.5. Telomerase

Telomerase is a reverse transcriptase enzyme that carries its own RNA molecule (with sequence "CCC AAU CCC" in vertebrates), which is used as a template when it elongates telomeres. In the examples reported below, telomerase was used to extend DNA sequences.

Ju and co-workers prepared a nanodevice for the sensitive detection of telomerase activity in order to distinguish normal cells from cancer cells.[88] These authors anchored a fluorescent quencher to the inner pore surfaces in MSNs and further loaded pores with fluorescein. Then the external surface of MSNs was functionalised with APTES and capped with a DNA sequence via electrostatic interactions, capable of activating telomerase (see Figure 8). This oligonucleotide sequence was extended in the presence of telomerase and deoxy-nucleoside triphosphate (dNTPs). When the DNA sequence was long enough, it formed a rigid hairpin and detached from MSNs, which resulted in fluorescein release. These MSNs were used for tracking intracellular telomerase activity in HeLa cells. In order to demonstrate telomerase responsive behaviour, HeLa cells were treated with different telomerase inhibitors (telomerase sense oligodeoxynucleotide, telomerase antisense oligodeoxynucleotide and epigallocatechingallate) and no cargo release was observed. Finally, the prepared nanoparticles were able to distinguish QSG-7701 liver cancer cells from BEL-7402 liver cells.

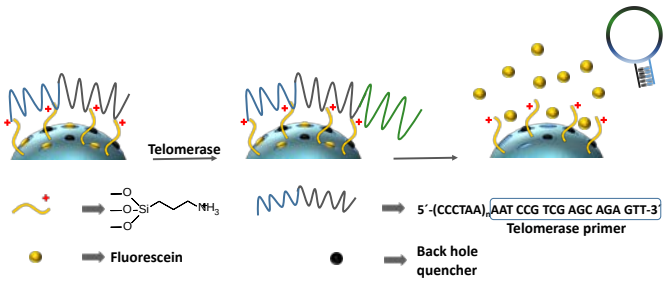

Figure 8. Telomerase-induced controlled fluorescein release from ssDNA-capped MSNs functionalised with a fluorescence quencher in the interior of pore walls.

Similarly, Lu and co-workers prepared a capped material to study telomerase activity with a glucometer. In this case, MSNs were loaded with glucose, functionalised with 3-(aminopropyl)trimethoxysilane and then capped with a single stranded DNA sequence through electrostatic interactions.[89] The glucometer signal showed linear dependence within the range of 100 to 5000 HeLa cells. The limit of detection was 80 HeLa cells mL^{-1}. In another paper, Cui and co-workers used a similar approach, but selected Au@Ag nanorods coated with a mesoporous silica shell as the inorganic support.[90] Mesoporous layer pores were loaded with DOX, and were then capped upon addition of a single DNA strand that contained a telomeric repeat complementary sequence and a telomerase substrate primer sequence. In the presence of telomerase, pores were uncapped and DOX was released. The authors were able to follow the uptake of the capped nanodevice in HeLa cells using SERS.

3.6.Miscellaneous

Huo and co-workers prepared MSNs functionalised with ferrocene moieties, which were sensitive to the redox changes induced by the presence of enzymes or by applying a voltage.[91] MCM-41 MSNs were prepared and their external surface was functionalised with APTES. In a second step, a ferrocene derivative that contained a carboxylic acid moiety was grafted onto the external surface by the formation of amide bonds. Finally, pores were loaded with Rh B and capped upon the addition of β-CDs (which formed inclusion complexes with grafted ferrocenes). The application of a +1.5V pulse oxidised ferrocene with the dethreading of the inclusion complex and subsequent cargo delivery. The combination of glucose, glucose oxidase (GOD) and horseradish peroxidase (HRP) also induced ferrocene oxidation and pore opening.

Wu and co-workers prepared NAD(P)H:quinone oxidoreductase 1 (NQO1)-responsive MSNs gated with a rotaxane nanovalve and loaded with Rh B or DOX.[92] Rotaxane was formed by coordinating α-CDs with a diethylene glycol stalk anchored to the surface of MSNs with a benzoquinone stopper. Enzyme NQO1 induced the reduction of benzoquinone with the subsequent stopper cleavage, which allowed a payload delivery. Delivery from DOX-loaded nanoparticles in cells with (i) high NQO1 expression (A549 and MCF-7 cells) and (ii) cells that lack enzyme NQO1 (HL-60 cells) was studied. Although both cell types internalised nanoparticles, the payload release was

observed only in the cells with a high NQO1 expression. The DOX-loaded system was demonstrated to inhibit tumour growth in mice.

Conclusions

We have herein reviewed the use of porous supports for controlled delivery applications based on employing enzymes. Enzyme-triggered gated materials are expected to offer remarkable applications in the biomedical field. So although there are a relatively large number of examples that use esterases, glycosidases, peptidases, reductases and DNases, this subfield in gated chemistry area has not yet been fully explored. Further advances will most likely take into account that the flow of certain biological processes relies on complex biochemical networks, along with the participation of multiple enzyme-dependent steps. Enzyme overexpression in certain diseases can be used to design personalised capped materials to be opened in a specific cell type and thus reduce undesirable side effects and increase the effectiveness of the delivered drug. Finally, the fact that synthetic molecules can be designed to contain both fragments recognised by target-enzymes and moieties for targeting certain cells, or for cell entry-control, also suggests that there is still plenty of room in this research area. Yet despite the exponential development of this field, drawbacks still need to be overcome. For instance, it must be recognised that in most published studies, delivered molecules are dyes/fluorophores used in an attempt to demonstrate the working mechanism of the gated ensemble, and fewer examples have been designed for real applications. Moreover, the potential bioaccumulation of MSNs or other porous supports when used *in vivo* is a subject that must be addressed, and more studies in this field must be carried out. By bearing all this in mind, new advances in the gated nanochemistry field using enzymes are anticipated in the near future.

Acknowledgements

Financial support from the Spanish Government and FEDER funds (Project MAT2015-64139-C4-1) and the Generalitat Valencia (Project PROMETEOII/2014/047) are gratefully acknowledged. A. Llopis-Lorente is grateful to "La Caixa" Banking Foundation for his PhD fellowship. B. Lozano-Torres is grateful to the Spanish Ministry of Economy and Competitiveness (MEC) for her FPU grant. Also A. Bernardos thanks the Spanish MEC for her Juan de la Cierva Contract.

Author information

Corresponding Author

*Ramón Martínez-Máñez (rmaez@qim.upv.es)

Biographies

Antoni LLopis is a PhD Student at the Universitat Politècnica de València (UPV) and his main area of interest lies in developing delivery systems and nanodevices using enzymes.

Beatriz Lozano is a PhD Student at the Universitat Politècnica de València (UPV) and her main area of interest lies in developing chemical probes based on gated nanomaterials for biomedical applications.

Andrea Bernardos is currently a researcher with a Juan de la Cierva Contract at the Universitat Politècnica de València, Spain. Her current research involves developing gated materials for advanced applications and drug delivery.

Félix Sancenón is Lecturer at the Universitat Politècnica de València and is co-author of more than 200 research publications. His current research interest comprises the use of hybrid materials to develop sensors and to construct molecular gates.

Ramón Martínez-Máñez is full Professor in the Department of Chemistry and is also the Director of the IDM Research Institute at the Universitat Politècnica de València and of the Biomedical Research Networking Center in Bioengineering, Biomaterials and Nanomedicine (CIBER-BBN). He is the co-author of more than 330 research publications and 22 patents. His current research involves designing gated hybrid materials for on-command delivery applications and developing new sensing methods for different chemicals of interest.

From left to right: Félix Sancenón, Andrea Bernardos, Ramón Martínez-Máñez, Beatriz Lozano-Torres and Antoni Llopis-Lorente.

Notes and references

1 L. Nicole, C. Laberty-Robert, L. Rozesa and C. Sanchez, *Nanoscale,* 2014, **12**, 6267-6292.
2 A. B. Descalzo, R. Martínez-Máñez, F. Sancenón, K. Hoffmann and K. Rurack, *Angew. Chem. Int. Ed.*, 2006, **45**, 5924-5948.
3 Q. Zhang, E. Uchaker, S. L. Candelariaza and G. Gao, *Chem. Soc. Rev.,* 2013, **42**, 3127-3171.
4 N. Linares, A. M. Silvestre-Albero E. Serrano, J. Silvestre-Albero and J. Carcía-Martínez, *Chem. Soc. Rev.,* 2014, **43**, 7681-7717.
5 T. Wagner, S. Haffer, C. Weinberger, D. Klaus and M. Tiemann, *Chem. Soc. Rev*., 2013, **42**, 4036-4053.
6 C. Perego and R. Millini, *Chem. Soc. Rev.,* 2013, **42**, 3956-3976.
7 A. E. Garcia-Bennett, *Nanomedicine,* 2011, **6**, 867-877.
8 E. Aznar, M. Oroval, L. Pascual, J. R. Murguía, R. Martínez-Máñez and F. Sancenón, *Chem. Rev.*, 2016, **116**, 561-718.
9 A. Stein, *Adv. Mater.*, 2003, **15**, 763.
10 G. J. A. A. Soler-Illia and O. Azzaroni, *Chem. Soc. Rev.*, 2011, **40**, 1107-1150.
11 A. P. Wight and M. E. Davis, *Chem. Rev.,* 2002, **102**, 3589-3614.
12 G. Kickelbick, *Angew. Chem. Int. Ed.,* 2004, **43**, 3102-3104.
13 S. Saha, K. C. -F. Leung, T. D. Nguyen, J. F. Stoddart and J. I. Zink, *Adv. Func. Mater.,* 2007, **17**, 685-693.

14 S. Angelos, E. Johansson, J. F. Stoddart and J. I. Zink, *Adv. Func. Mater.,* 2007, **17**, 2261-2271.
15 F. Wang, X. Liu and I. Willner, *Angew. Chem. Int. Ed.,* 2015, **54**, 1098-1129.
16 N. Song and Y. -W. Yang, *Chem. Soc. Rev.,* 2015, **44**, 3474-3504.
17 G. Wang and J. J. Zhang, *Photochem. Photobiol. C, Photochem. Rev.,* 2012, **13**, 299-309.
18 A. B. Braunschweig, B. H. Northrop and J. F. Stoddart, *J. Mater. Chem.,* 2006, **16**, 32-44.
19 B. G. Trewyn, S. Giri, I. I. Slowing and V. S. -Y. Lin, *Chem. Commun.*, 2007, 3236-3245.
20 E. Aznar, R. Martínez-Máñez and F. Sancenón, *Expert Opin. Drug Deliv*., 2009, **6**, 643-655.
21 Y. –W. Yang, *Med. Chem. Commun.*, 2011, **2**, 1033-1049.
22 a) F. Sancenón, Ll. Pascual, M. Oroval, E. Aznar and R. Martínez-Máñez, *ChemOpen*, 2015, **4**, 418-437; b) Y. –W. Yang, Y. –L. Sun and N. Song, *Acc. Chem. Res.*, 2014, **47**, 1950-1960.
23 H. P. Rim, K. H. Min, H. J. Lee, S. Y. Jeong and S. C. Lee, *Angew. Chem.*, *Int. Ed.* 2011, **50**, 8853-8857.
24 P. Liu, X. Wang, K. Hiltunen and Z. Chen, *ACS Appl. Mater. Interfaces*, 2015, **7**, 26811-26818.
25 S. Datz, C. Argyo, M. Gattner, V. Weiss, K. Brunner, J. Bretzler, C. von Schirnding, A. A. Torrano, F. Spada, M. Vrabel, H. Engelke, C. Bräuchle, T. Carrel and T. Bein, *Nanoscale*, 2016, **8**, 8101-8110.
26 M. Chen, C. Huang, C. He; W. Zhu, Y. Xu and Y. Lu, *Chem. Commun.*, 2012, **48**, 9522-9524.
27 a) E. Aznar, R. Villalonga, C. Giménez, F. Sancenón, M. D. Marcos, R. Martínez-Máñez, P. Díez, J. M. Pingarrón and P. Amorós, *Chem. Commun.*, 2013, **49**, 6391-6393; b) M. Oroval, P. Díez, E. Aznar, C. Coll, M. D. Marcos, F. Sancenón, R. Villalonga and R. Martínez-Máñez*, Chem. Eur. J.*, 2017, **23**, 1353-1360.
28 W. Zhao, H. Zhang, Q. He, Y. Li, J. Gu, L. Li, H. Li and J. Shi, *Chem. Commun*., 2011, **47**, 9459-9461.
29 P. Díez, A. Sánchez, M. Gamella, P. Martínez-Ruiz, E. Aznar, C. de la Torre, J. R. Murguia, R. Martínez-Máñez, R. Villalonga and J. M. Pingarrón, *J. Am. Chem. Soc.*, 2014, **136**, 9116-9123.
30 P. Díez, A. Sánchez, C. de la Torre, M. Gamella, P. Martínez-Ruíz, E. Aznar, R. Martínez-Mañez, J. M. Pingarrón and R. Villalonga, *ACS Appl. Mater. Interfaces,* 2016, **8**, 7657-7665.
31 X. X. Sun, Y. N. Zhao, V. S. Y. Lin, I. I. Slowing and B. G. Trewyn, *J. Am. Chem. Soc.*, 2011, **133**, 18554-18557.
32 R. Villalonga, P. Díez, A. Sánchez, E. Aznar, R. Martínez-Máñez and J. M. Pingarrón, *Chem. Eur. J.*, 2013, **19**, 7889-7894.
33 X. Wang, P. Liu, Z. Chen and J. Shen, *RSC Adv.*, 2016, **6**, 25480-25484.
34 L. Pascual, S. El Sayed, R. Martínez-Mañez, Ana M. Costero, S. Gil, P. Gaviña and F. Sancenón, *Org. Lett.*, 2016, **18**, 5548-5551.
35 H. Zhou, X. Wang, Jun Tang and Y. –W. Yang, *Polymers*, 2016, **8**, 277.
36 P. D. Thornton and A. Heise, *J. Am. Chem. Soc.,* 2010, **132**, 2024-2028.
37 A. Schlossbauer, J. Kecht and T. Bein, *Angew. Chem. Int. Ed.,* 2009, **48**, 3092-3095.
38 N. Singh, A. Karambelkar, L. Gu, K. Lin, J. S. Miller, C. S. Chen, M. J. Sailor and S. N. Bhatia, *J. Am. Chem. Soc.* 2011, **133**, 19582-19585.
39 X. J. Yang, F. Pu, C. E. Chen, J. S. Ren and X. G Qu, *Chem. Commun.,* 2012, **48**, 11133-11135.
40 C. de la Torre, I. Casanova, G. Acosta, C. Coll, M. J. Moreno, F. Albericio, E. Aznar, R. Mangues, M. Royo, F. Sancenón and R. Martínez-Máñez, *Adv. Funct. Mater.,* 2015, **25**, 687-695.
41 S. H. van Rijt, D. A. Bölükbas, C. Argyo, S. Datz, M. Lindner, O. Eickelberg, M. Königshoff, T.Bein and S. Meiners, *ACSNano*, 2015, **9**, 2377-2389.
42 A. Tukkapa, A. Ultimo, C. de la Torre, T. Pardo, F. Sancenón and R. Martínez-Mañez, *Langmuir*, 2016, **32**, 8507-8515.
43 C. Coll, L. Mondragón, R. Martínez-Máñez, F. Sancenón, M. D. Marcos, J. Soto, P. Amorós, E. Pérez-Payá, *Angew. Chem. Int. Ed.,* 2011, **50**, 2138-2140.
44 C. de la Torre, L. Mondragón, C. Coll, F. Sancenón, M. D. Marcos, R. Martínez-Máñez, P. Amorós, E. Pérez-Payá and M. Orzaez, *Chem. Eur. J.,* 2014, **20**, 15309-15314.
45 J. M. Li, F. Liu, Q. Shao, Y. Z. Min, M. Costa, E. K. L. Yeow and B.G. Xing, *Adv. Healthc. Mater.,* 2014, **3**, 1230-1239.
46 Y. -J. Cheng, G. -F. Luo, J. -Y. Zhu, X. -D. Xu, X. Zeng, D. -B. Cheng, Y. -M. Li, Y. Wu, X. -Z. Zhang, R. -X. Zhuo and H. Feng, *ACS Appl. Mater. Interfaces*, 2015, **7**, 9078-9087.
47 K. Radhakrishnan, S. Gupta, D. P. Gnanadhas, P. C. Ramamurthy, D. Chakravortty and A. M. Raichur, *Part. Part. Syst. Charact*., 2014, **31**, 449-458.
48 J. Zhang, Z. -F. Yuan, Y. Wang, W. -H. Chen, G. -F. Luo, S.-X. Cheng, R. -X. Zhuo and X. -Z. Zhang., *J. Am. Chem. Soc.* 2013, **135**, 5068-5073.
49 J. H. Xu, F. P. Gao, L. L. Li, H. L. Ma, Y. S. Fan, W. Liu, S. S. Guo, X. Z. Zhao and H. Wang, *Micropor. Mesopor. Mater.,* 2013, **182**, 165-172.
50 Y. Liu, X. Ding, J. Li, Z. Luo, Y. Hu, J. Liu, L. Dai, J. Zhou, C. Hou and K. Cai, *Nanotechnology*, 2015, **26**, 145102-145116.
51 J. Liu, B. Zhang, Z. Luo, X. Ding, J. Li, L. Dai, J. Zhou, X. Zhao, J. Ye and K. Cai, *Nanoscale*, 2015, **7**, 3614-3626.
52 J. Hu, L- Liu, Z.-Y. Li, R.-X. Zhuo and X.-Z Zhang, *J. Mater. Chem. B*, 2016, **4**, 1932-1940.
53 L. Mondragón, N. Mas, V. Ferragud, C. de la Torre, A. Agostini, R. Martínez-Máñez, F. Sancenón, P. Amorós, E. Pérez-Payá and M. Orzaez, *Chem. Eur. J.,* 2014, **20**, 5271-5281.
54 I. Candel, E. Aznar, L. Mondragón, C. de la Torre, R. Martínez-Máñez, F. Sancenón, M. D. Marcos, P. Amorós, C. Guillem, E. Pérez-Payá and A. Costero, *Nanoscale*, 2012, **4**, 7237-7245.
55 A. Agostini, L. Mondragón, C. Coll, E. Aznar, M. D. Marcos, R. Martínez-Máñez, F. Sancenón, J. Soto, E. Pérez-Payá and P. Amorós. *ChemistryOpen*, 2012, **1**, 17-20.
56 A. Popat, S. Jambhrunkar, J. Zhang, J. Yang, H. Zhang, A. Meka and C. Yu, *Chem. Commun.*, 2014, **50**, 5547-5550.
57 R. Bhat, A. Ribes, N. Mas, E. Aznar, F. Sancenón, M. D. Marcos, J. R. Murguía, A. Venkataraman and R. Martínez-Mañez, *Langmuir*, 2016, **32**, 1195-2000.
58 C. de la Torre, L. Mondragón, C. Coll, A. García, F. Sancenón, R. Martínez-Mañez, P. Amorós, E. Pérez-Payá and M. Orzáez, *Chem. Eur. J.*, 2015, **21**, 15506-15510.
59 K. Patel, S. Angelos, W. R. Dichtel, A. Coskun, Y. W. Yang, J. I. Zink and J. F. Stoddart, *J. Am. Chem. Soc.* 2008, **130**, 2382-2383.
60 Y. Klichko, N. M. Khashab, Y. W. Yang, S. Angelos, J. F. Stoddart and J. I. Zink, *Micropor. Mesopor. Mater.* 2010, **132**, 435-441.
61 F. Porta, G. E. M. Lamers, J. Morrhayim, A. Chatzopoulou, M. Schaaf, H. den Dulk, C. Backendorf, J. I. Zink and A. Kros, *Adv. Healthc. Mater.* 2013, **2**, 281-286.
62 A. Agostini, L. Mondragón, L. Pascual, E. Aznar, C. Coll, R. Martínez-Máñez, F. Sancenón, J. Soto, M. D. Marcos, P. Amorós, A. M. Costero, M. Parra and S. Gil, *Langmuir*, 2012, **28**, 14766-14776.
63 A. Bernardos, L. Mondragón, I. Javakhishvili, N. Mas, C. de la Torre, R. Martínez-Máñez, F. Sancenón, J. M. Barat, S. Hvilsted, M. Orzaez, E. Pérez-Payá and P. Amorós, *Chem. Eur. J.*, 2012, **18**, 13068-13078.
64 Y. L. Sun, Y. Zhou, Q. L. Li, Y. W. Yang, *Chem. Commun.*, 2013, **49**, 9033-9035.

65 X. Chen, A. H. Soeriyadi, X. Lu, S. M. Sagnella, M. Kavallaris and J. J. Gooding, *Adv. Funct. Mater.* 2014, **24**, 6999-7006.
66 Z. Liu, X. Chen, X. Zhang, J. J. Gooding and Y. Zhou, *Adv. Healthcare Mater.* 2016, **5**, 1401-1407.
67 N. Mas, D. Arcos, L. Polo, E. Aznar, S. Sanchez-Salcedo, F. Sancenón, A. Garcia, M. D. Marcos, A. Baeza, M. Vallet-Regí and R. Martínez-Máñez, *Small* 2014, **10**, 4859-4864.
68 Y. F. Zhu, W. J. Meng and N. Hanagata, *Dalton Trans.*, 2011, **40**, 10203-10208.
69 G. L. Zhang, M. L. Yang, D. Q. Cai, K. Zheng, X. Zhang, L. F. Wu and Z. Y. Wu, *ACS Appl. Mater. Inter.*, 2014, **6**, 8042-8047.
70 Z. Zhang, D. Balogh, F. Wang, S. Y. Sung, R. Neuchsthai and I. Willner, *ACS Nano*, 2013, **7**, 8455-8468.
71 A. Bernardos, E. Aznar, M. D. Marcos, R. Martínez-Máñez, F. Sancenón, J. Soto, J. M. Barat and P. Amorós, *Angew. Chem. Int. Ed.,* 2009, **48**, 5884-5887.
72 A. Bernardos, L. Mondragón, E. Aznar, M. D. Marcos, R. Martínez-Máñez, F. Sancenón, J. Soto, J. M. Barat, E. Pérez-Payá and C. Guillem, *ACS Nano,* 2010, **4**, 6353-6368.
73 C. Acosta, E. Pérez-Esteve, C. A. Fuenmayor, S. Benedetti, M. S. Cosio, J. Soto, F. Sancenón, S. Mannino, J. Barat and M.D Marcos, *ACS Appl. Mater. Inter*., 2014, **6**, 6453-6460.
74 A. Agostini, L. Mondragón, A. Bernardos, R. Martínez-Máñez, M.D Marcos, F. Sancenón, J. Soto, A. Costero, C. Manguán-García and R. Perona, *Angew.Chem. Int. Ed.,* 2012, **51**, 10556-10560.
75 W. Guo, C. Yang, L. Cui, H. Lin and F. Qu, *Langmuir,* 2014, **30**, 243-249.
76 Z. W. Chen, Z. H. Li, Y. H. Lin, M. L. Yin, J. S. Ren and X. G. Qu, *Chem. Eur. J.,* 2013, **19**, 1778-1783.
77 M. L. Yin, E. G. Ju, Z. W. Chen, Z. H. Li, J. S. Ren and X. G. Qu, *Chem. Eur. J.,* 2014, **20**, 14012-14017.
78 Z. Wang, Z. Chen, Z. Liu, P. Shi, K. Dong, E. Ju, J. Ren and X. A. Qu, *Biomater.,* 2014, **35**, 9678-9688.
79 Q. Zhao, J. Liu, W. Zhu, C. Sun, D. Di, Y. Zhang, P. Wang, Z. Wang and S. Wang, *Acta Biomater.*, 2015, **23,** 147-156.
80 C. Yang, W. Guo, N. An, L. Cui, T. Zhang, R. Tong, Y. Chen, H. Lin and F. Qu, *RSC Adv.*, 2015, **5**, 80728-80738.
81 X. Chen and Z. Liu, *Macromol. Rapid Commun.*, 2016, **37,** 1533-1539.
82 A. Hakeem, R. Duan, F. Zahid, C. Dong, B. Wang, F. Hong, X. Ou, Y. Jia, X. Lou and F. Xia, *Chem. Commun.,* 2014, **50**, 13268-13271.
83 C. Park, H. Kim, S. Kim and C. Kim, *J. Am. Chem. Soc.,* 2009, **131**, 16614-16615.
84 C. Giménez, E. Climent, E. Aznar, R. Martínez-Mánez, F. Sancenón, M. D. Marcos, P. Amorós and K. Rurack, *Angew. Chem. Int. Ed.,* 2014, **53**, 12629-12633.
85 A. Hakeem, F. Zahid, R. Duan, M. Asif, T. Zhang, Z. Zhang, Y. Cheng, Z. Lou and F. Xia, *Nanoscale*, 2016, **8**, 5089-5097.
86 N. Mas, A. Agostini, L. Mondragón, A. Bernardos, F. Sancenón, M.D. Marcos, R. Martínez-Máñez, A. Costero, S. Gil and M. Merino-Sanjuan, *Chem. Eur. J.,* 2013, **19**, 1346-1356.
87 X. Li, T. Tang, Y. Zhou, Y. Zhang and Y. Sun, *Micropor. Mesopor. Mater.*, 2014, **184**, 83-89.
88 R. Qian, L. Ding and H. Ju, *J. Am. Chem. Soc.* 2013, **135**, 13282-13285.
89 Y. Wang, M. Lu, J. Zhu and S. Tian, *J. Mater. Chem. B*, 2014, **2**, 5847-5853.
90 S. Zong, Z. Wang, H. Chen, D. Zhu, P. Chen and Y. Cui, *IEEE Trans. Nanobiosci.*, 2014, **13**, 55-60.
91 Y. Xiao, T.Wang, Y. Cao, X. Wang, Y. Zhang, Y. Liu and Q. Huo, *Dalton Trans.*, 2015, **44**, 4355-4361.
92 S. Reddy Gayam, P. Venkatesan, Y. M. Sung, S. Y. Sung, S. H. Hu, H. Y. Hsu and S. P. Wu, *Nanoscale*, 2016, **8**, 12307-12317.